

MODAL TEST CORRELATION AND ERROR LOCALIZATION FOR FINITE ELEMENT MODELS OF SPACECRAFT STRUCTURES

J. López-Díez[♦], V. Marco-Gómez[⊗], C. Cuerno-Rejado[♦]

Universidad Politécnica de Madrid, E.T.S.I. Aeronáuticos,

Pza. Cardenal Cisneros 3, 28040 Madrid. Spain

Pedro Luengo[†]

C.A.S.A. División Espacio, Avda. de Aragón 404, 28022 Madrid. Spain.

ABSTRACT

This paper describes the use of some tools for matching modal test data and finite element model results. Different reduction/expansion techniques have been implemented in order to become analytical and experimental models size compatible. MAC, NCO and SCO coefficients allow quantifying the degree of correlation between analysis and test results. An error localisation technique based on Mass and Stiffness Baruch's method updating has been implemented. The analytical model of the structure is updated on the basis of experimental data using a direct updating method and new stiffness and mass matrices are generated. The error vector technique assigns errors calculated on stiffness and mass matrices to the different elements of the model. Thence, they are plotted on the mesh, and its colour denotes the amount of error. The process of error interpretation is simplified and physical meaning can be deduced. Modes measured in tests are expanded and plotted and visual comparison of mode shapes (analytical determined and experimentally measured) is performed. The influences of the boundary conditions simulation and sensor location are investigated.

Algorithms to calculate different correlation parameters, reduction/expansion methods and tools for error location have been implemented in DMAP. Therefore, they can be included in most of the finite element models developed in MSC/NASTRAN. The visualisation on the model results useful in order to identify the major modelling error regions. A study on a flat plate is used as benchmark. Finally, results of the application to the Polar Platform Panel model are showed.

[♦] Associate Professor, Departamento de Vehículos Aeroespaciales, Universidad Politécnica de Madrid.

[⊗] Assistant Professor, Departamento de Vehículos Aeroespaciales, Universidad Politécnica de Madrid.

[†] Senior Structural Dynamics Engineer, C.A.S.A, Structural Analysis Department.

I. Introduction

Obtaining highly accurate finite element models is necessary for predicting the performance of spacecraft structures. To localise and quantify modelling errors modal test data are used to revise the analytical model. This task is known as model update or test/analysis correlation. In spite of the experience of the structural engineers, finite element models have usually sufficient freedom, for example in the modelling of the joints or the boundary conditions, to allow the updating of modelling uncertainties. Most of the techniques attempt to modify stiffness and/or mass matrices such that the mode shapes and frequencies of the model closely match experimentally measured modal parameters.

A great amount of literature exists about model update. The methods proposed generally fall within three classes: optimal matrix updating, sensitivity-based parameters updating and eigenstructure assignment¹. An overview of these techniques is provided in different publications^{1, 2, 3}. These techniques seek a reviewed finite element model whose modal properties are in agreement with those from an experimental modal analysis of the structure. Several difficulties still remain on these approaches: distinguishing between stiffness and inertia error in most model update algorithms; selecting which modes to use in the update and determining modal correspondence (for a complex structure as the one of a spacecraft, this correspondence is difficult to determine); the difficulty arising because of the number of measurement degrees of freedom (DOF) is much smaller than the number of analytical DOF. Problems are often encountered due to errors introduced by the expansion process and from the smearing effect on modelling errors introduced by model reduction^{4, 5}. For large spacecraft structural models these inconveniences get worse because of the difficulties in interpreting the results^{6, 7}.

The present paper presents a methodology to correlate analytical and experimental results based on the computation of a great variety of correlation coefficients, using different expansion processes. Error location methodology is based on the computation of mass and stiffness error matrices. The error is transferred to the analytical degrees of freedom through the error vector⁸⁹, and then plotted on the structure. This allows identifying the sources of the errors and physical meaning can be deduced. Engineer judgement can valorise if results are (or not) adequate. A free-free flat plate of composite illustrates the method proposed. For this very simple example, the structural finite element model is well known, and the only uncertainties in the stiffness matrix come from the boundary conditions simulations; mass error matrix must point out the presence of the sensors. Finally, the capability of the method to be used in large FEM models is demonstrated by its application to the Polar Platform Panel structural model.

II. Correlation process

Mode pairing

Previously to any operation to assess the quality of the analytical model, to establish a correspondence between analytical and measured modes is required. Frequency proximity is usually an adequate clue, but a mode shape comparison is recommended. Several parameters can be used to correlate analytical and experimental modes¹⁰: modal scale factor (MSF), orthogonality (OR), cross-orthogonality (XOR), modal effective mass (MEM)¹¹, modal assurance criterion (MAC)¹², normalized cross orthogonality (NCO)¹³, SEREP based cross-orthogonality (SCO)¹⁴...

Modal assurance criterion (MAC) is the parameter most often used. To calculate MAC, the first approach is to reduce the analytical mode shapes to the order of the experimental model. Components of the analytical modal vectors are partitioned into two sets: the measured degrees of freedom set and the slave degrees of freedom set. In order to pair analytical and experimental mode shapes, MAC matrix is calculated comparing experimental mode shapes versus the set of master degrees of freedom corresponding to the analytical modal matrix. This criterion calculates the least square deviation about a straight line of the plot of two arbitrarily scaled mode shapes. This is defined in equation (1).

$$MAC(i, j) = \frac{\left| \{ \mathbf{f}_X \}_i^T \{ \mathbf{f}_{A_m} \}_j \right|^2}{\left(\{ \mathbf{f}_X \}_i^T \{ \mathbf{f}_X \}_i \right) \left(\{ \mathbf{f}_{A_m} \}_j^T \{ \mathbf{f}_{A_m} \}_j \right)} \quad (1)$$

being $\{ \mathbf{f}_X \}_i$ the i -th experimental mode. Each analytical mode shape is partitioned into two different sets: master and slave degrees of freedom as follows:

$$\{ \mathbf{f}_A \}_j = \begin{Bmatrix} \mathbf{f}_{A_m} \\ \mathbf{f}_{A_s} \end{Bmatrix}_j \quad (2)$$

For the purposes of this paper, the master degrees of freedom are the measured one in the modal tests.

Expansion/reduction techniques

The error location process used in the present work requires expanding the experimental results to the size of the analytical model, or reducing the analytical model to the measured degrees of freedom. The technique used for the identification of the sources of discrepancies between tests and analysis recommends expanding the experimental results.

Reduction/expansion techniques have been studied since sixties¹⁵. Static reduction¹⁶ is the most widely used. This work was the forerunner of a series of technique based on the balance of the equation of the motion; dynamic reduction^{17,18,19,20...} (on its different versions) and improved reduction system²¹ (IRS) are the most known. The last one has been proved to be efficient for large spacecraft structures²².

All these techniques express the whole set of degrees of freedom, $\{q\}$, as a transformation on a sub-set of degrees of freedom (master degrees of freedom), $\{q_m\}$, through a matrix of transformation, $[T]$.

$$\{q\} = \begin{Bmatrix} q_m \\ q_s \end{Bmatrix} = [T] \{q_m\} = \begin{bmatrix} I \\ T_{sm} \end{bmatrix} \{q_m\} \quad (3)$$

Another kind of reduction/expansion technique obtains the matrix of transformation using the mode shapes, as modal reduction²³ or “system equivalent reduction expansion process” (SEREP)²⁴.

Hybrid techniques use together these two philosophies to obtain the matrix of transformation^{25,26,27,28,29}. Finally, system-balancing techniques could be also implemented.

Most of these techniques have been implemented in MSC/NASTRAN^{30,31}.

In the present work, results using Guyan, IRS and SEREP techniques are presented. To select the appropriate expansion technique MAC, NCO and SCO correlation technique have been used. MAC is calculated both with Guyan and IRS. A Guyan expansion of experimental modes is also used for NCO calculations. Finally, SEREP expansion is checked through the calculation of the SCO as defined below.

The normalised cross orthogonality (NCO) is basically the MAC coefficient weighted by a partition of the global mass or stiffness matrix. This is defined in Eq. 4.

$$NCO(i, j) = \frac{\left| \{f_X\}_i^T [M_A] \{f_A\}_j \right|^2}{\{f_X\}_i^T [M_A] \{f_X\}_i \cdot \{f_A\}_j^T [M_A] \{f_A\}_j} \quad (4)$$

To calculate the NCO it is necessary to use the analytical mass matrix, $[M_A]$. Generally spoken, the measured degrees of freedom are less numerous than the analytical model contains, it is necessary to adapt one data set. It is possible to reduce the mass matrix to the measured degrees of freedom or to expand the measured modes to the degrees of freedom of the analytical model. The distinct methods to carry out these operations (expansion or reduction) influence the result of the NCO. Static expansion has been applied in the results presented in this paper.

MAC and NCO values close to one observe a good correlation between modes and a poor correlation corresponds to values close to zero. However, this technique has been found inappropriate for some applications and a SEREP theoretical mass reduced based normalised cross orthogonality (SCO) correlation coefficient (5) can be used instead¹⁴.

$$SCO(i, j) = \frac{\left| \{f_{X_{SEREP}}\}_i^T [M_A] \{f_A\}_j \right|^2}{\left(\{f_{X_{SEREP}}\}_i^T [M_A] \{f_{X_{SEREP}}\}_i \right) \cdot \left(\{f_A\}_j^T [M_A] \{f_A\}_j \right)} \quad (5)$$

Where the experimental modes have been expanded using the SEREP method. This correlation coefficient has an advantage over MAC that it is more sensitive to the actual similarity or dissimilarity between the mode shapes. SCO will generally have a higher value for two similar mode shapes than MAC correlation coefficient, and conversely for two dissimilar mode shapes, SCO will have a lower value than MAC.

The expansion technique used in the error location process will be the one presenting the best quality in the correlation.

III. Error localisation process

For large structural finite element models which present discrepancies with the measured experimental results, previous to update the model, it is adequate to localize the origin of this errors, instead of a global updating. For this purpose, an error location technique has been implemented. The Baruch's methods³² are used to calculate the Updated Stiffness and Mass matrixes, K_{UP} and M_{UP} .

Comparing these updated matrices with the original ones, error matrices \mathbf{DK} and \mathbf{DM} are calculated as shown in Eq. 6 and 7, which will be used for data extraction in order to calculate the error distribution to be displayed on the structure.

$$\Delta K_{ij} = \frac{\left(K_{UP_{ij}} - K_{a_{ij}}\right)^2}{K_{a_{ij}}^2} \quad (6)$$

$$\Delta M_{ij} = \frac{\left(M_{UP_{ij}} - M_{a_{ij}}\right)^2}{M_{a_{ij}}^2} \quad (7)$$

From each of these matrixes (i.e. \mathbf{DK}) the Error Vector (VK_{ERROR} for stiffness and VM_{ERROR} for mass) will be defined. An element “ i -th” of the vector V_{ERROR} is calculated by summing up all elements of the concerned column “ i -th” indicated in the Error Matrix, \mathbf{DK} :

$$VK_{ERRORi} = \sum_j \Delta K_{ij} \quad (8)$$

In this way all errors related to the “ i -th” degree of freedom are collected in one number, which corresponds to a global degree of freedom of a grid point (i.e. translation or rotation in one sense) in the finite element model. The size of the error vector is the one corresponding to the number of degrees of freedom of the finite element model. Therefore, each component of the vector is associated with a node displacement direction. The errors in the mass distribution are calculated in a similar way.

The errors obtained with the methods described are displayed on the structure. These methods serve to compare different cases of the same finite element model, while it allows easy interpretation and the presentation is conveniently arranged.

The capabilities of the implemented method are showed by its application to the study of the behaviour of a very simple model, used as a benchmark. A composite free-free plate has been selected to this purpose. In this example, the influence of the identification of the accelerometer situation is showed. Error distributions corresponding to the mass and stiffness are easy to explain because the only uncertainties are the boundary condition (free-free) simulation and accelerometers masses. As final conclusion, results on a large spacecraft real structure, the Polar Platform Panel, are presented.

IV. Free-free composite plate.

Description of the plate

Figure 1 sketches the tested configuration. The test specimen consists in a plate of 386x600 mm. The plate has two skins and a core. Skins (0,39 mm thickness) are manufactured on XN 50/RS 3: [-60°,0°,60°]. Skins are cured apart from the core, and then, bonded to it with BSL- 312L. Core material designation is NIDA 4-20 (5056-3/16-0.007-2.0) and it is 15 mm of thickness. The measured mass of the plate is 0,478 kg.

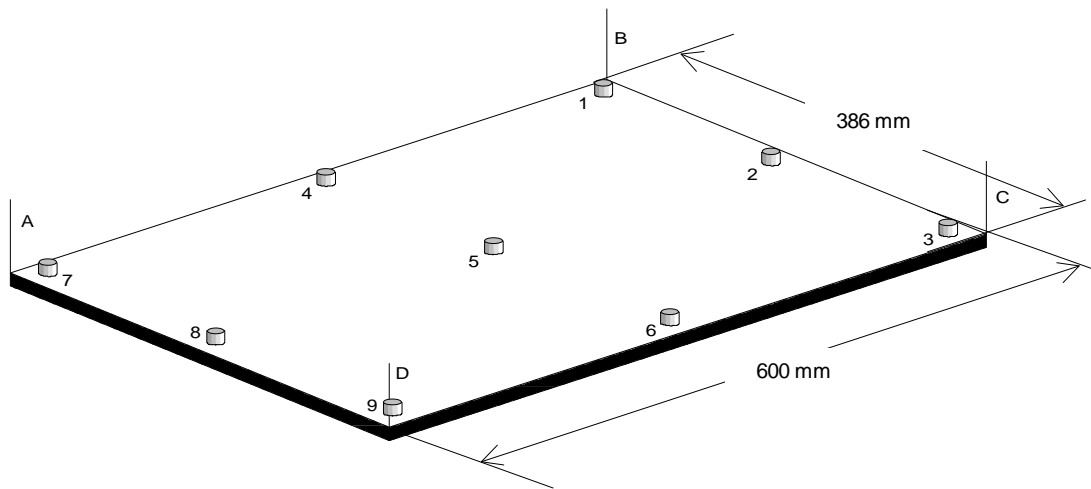


Figure 1. Flat plate manufactured in composite. The plate is hinged by the corners with elastic ropes (A, B, C, D). The location of the accelerometers is depicted.

Structural properties are modulus of elasticity: $E= 61,7 \text{ GN/m}^2$; Poisson's ratio $\nu=0,3$; and mass per unit area of plate, $\rho= 2,064 \text{ kg/m}^2$. The aspect ratio of this plate is $L=a/b=1,5$. This configuration was chosen because of it is well reported³³.

A campaign of modal analysis tests was carried out to determine experimentally the mode shapes and modal frequencies. The plate was suspended with four elastic ropes bonded to the corners. Two different instrumentation layouts were used. The first consists in nine low mass accelerometers located (see Fig. 1) approximately in the middle of the plate, in the corners and in the middle of each side; the mass of each accelerometer is 0,007 kg. A modal test was repeated using only the four accelerometers located at the corners. Results are reported for the two configurations in this work.

Finite element model

A code in MSC/NASTRAN v68.2 allows to analysis the structure above described. The structural model reproduces the state of the middle plane of the plate assuming a bidimensional

stress state. Only CQUAD4 elements form the structural model, with no restrictions to reproduce a free-free configuration. The grid is of twenty elements in width and thirteen in length, with a total of two hundred and sixty elements. Square elements of 30 mm are employed in the twelve first rows. The last row is formed with rectangular elements of 30 mm in width and 26 mm in length. Annex A presents the bulk data corresponding to the plate.

Concentrated masses of 0,007 kg are used to simulate the mass of the accelerometers. These masses were assigned on the nearest grid point. Also, an study of the influence of the accelerometer location was carried out. RBAR element connects a grid representing the accelerometer sensor position with the nearest grid. This model simulates the actual output of the accelerometers.

Results

Table 1 shows the eigenfrequencies measured in the tests. Data corresponding to the nine and four accelerometer configuration are presented. Modal analysis software performs the calculation of mode shapes, frequencies, modal damping, modal mass and generalised stiffness.

Table 1a. Experimental frequencies. Nine accelerometers instrumented the plate.

Mode n°	No of sensors	Freq Hz	Damping %	Mass kg	Damping kg/s	Gen. Stiffness Kg/s ²
1	9	296,86	0,89	0,079	2,61	2,75x10 ⁵
2	9	332,09	0,89	0,151	5,60	6,56x10 ⁵
3	9	627,76	0,53	0,094	3,91	1,46x10 ⁶
4	9	810,60	1,38	0,148	20,8	3,48 x10 ⁶
5	9	867,88	1,54	0,004	0,68	1,21 x10 ⁵
6	9	925,03	0,26	0,447	13,4	1,51 x10 ⁷

Table 1b. Experimental frequencies. Four accelerometers instrumented the plate.

Mode n°	No of sensors	Freq Hz	Damping %	Mass kg	Damping kg/s	Gen. Stiffness Kg/s ²
1	4	296,99	0,97	0,077	2,77	2,67 x10 ⁵
2	4	349,30	0,95	0,128	5,31	6,16 x10 ⁵
3	4	653,21	0,45	0,089	3,29	1,51 x10 ⁶
4	4	846,32	1,15	0,147	18,0	4,16 x10 ⁶
5	4	947,78	1,43	0,150	25,7	5,33 x10 ⁶

Correlation results are showed in tables 2 to 3. For the shake of simplicity, only correlation corresponding to the first experimental modes is listed. Table 2 depicts correlation parameters of the plate tested with nine accelerometers. Table 3 depicts correlation parameters of the plate tested with four accelerometers. Accelerometers location is discussed comparing a and be versions of the tables..

Table 2a. Correlation Parameters. Nine accelerometers at the middle plane.

```
.dat
LO NASTRAN: 9 CONM2 (7 gr.) en el plano medio de la placa
      QUAD4 V67.5
      Lumped mass matrices
: 9 acel.
```

P A R A M E T R O S D E C O R R E L A C I O N
P A R A
6 MODOS EXPERIMENTALES Y
6 MODOS ANALITICOS

TEST NO. 1, FRECUENCIA (HZ) = 2.968600E+02

ANAL. NO.	MAC	MAC GST	MAC GPS	NCO	SCO
1	9.708119E-01	5.573452E-02	3.623066E-02	1.003434E-01	9.799199E-01
2	4.663402E-03	2.540114E-02	8.457935E-02	1.185489E-02	6.301622E-03
3	1.350533E-03	1.959415E-02	6.088862E-05	4.437969E-04	1.665720E-03
4	3.709915E-05	1.751660E-01	6.124688E-02	2.900030E-02	7.482434E-05
5	5.386100E-04	1.189652E-01	2.982606E-02	4.878926E-03	1.946582E-03
6	2.774164E-03	7.664806E-02	2.649864E-01	2.212063E-01	1.009133E-02

EST NO. 2, FRECUENCIA (HZ) = 3.320900E+02

ANAL. NO.	MAC	MAC GST	MAC GPS	NCO	SCO
1	2.072025E-02	1.524438E-01	4.237962E-02	2.036945E-01	1.649382E-02
2	9.639886E-01	1.531309E-02	4.819861E-02	5.468898E-03	9.818012E-01
3	1.895535E-04	5.384960E-03	2.225260E-02	1.218808E-03	1.188225E-04
4	3.715810E-02	1.007067E-01	5.858323E-02	4.623637E-03	6.192833E-04
5	2.891820E-05	7.805154E-02	4.676175E-02	1.042638E-04	3.153430E-05
6	2.395676E-03	3.063739E-02	1.721468E-01	1.012554E-01	9.353941E-04

Table 2b. Correlation Parameters. Nine accelerometers at real location.

```
aset.dat
```

LO NASTRAN: 9 RBAR de 13 mm
 9 CONM2 (7 gr.) en el extremo de las RBAR
 QUAD4 V67.5
 Lumped mass matrices
 : ASET gdl experimentales 9 aceler

 P A R A M E T R O S D E C O R R E L A C I O N
 P A R A
 5 MODOS EXPERIMENTALES Y
 6 MODOS ANALITICOS

EST NO. 1, FRECUENCIA (HZ) = 2.968600E+02

ANAL. NO.	MAC	MAC GST	MAC GPS	NCO	SCO
1	9.992000E-01	1.706039E-02	1.003070E-04	2.214865E-02	9.991301E-01
2	1.247721E-03	7.522094E-03	2.644655E-03	5.496906E-02	7.805541E-04
3	2.151923E-04	5.218472E-02	4.037185E-02	2.414042E-02	1.666955E-05
4	8.756445E-05	1.558549E-01	9.283751E-02	9.719419E-02	1.700930E-06
5	5.246512E-04	8.148841E-02	5.907858E-02	4.126239E-02	2.584092E-06
6	2.804151E-04	1.014616E-01	1.606397E-02	2.044838E-02	6.838736E-05

EST NO. 2, FRECUENCIA (HZ) = 3.320900E+02

ANAL. NO.	MAC	MAC GST	MAC GPS	NCO	SCO
1	1.139436E-03	6.836498E-02	2.315927E-03	4.207322E-02	1.650459E-03
2	9.977918E-01	2.449900E-02	5.836308E-03	6.307541E-03	9.982136E-01
3	1.043114E-03	5.204611E-02	1.764919E-02	2.079663E-04	1.279599E-05
4	4.736736E-02	5.272857E-04	1.157069E-01	2.992101E-02	2.747195E-05
5	5.053832E-06	2.661407E-04	1.052870E-01	4.500387E-02	1.116349E-06
6	5.911896E-03	7.714560E-02	9.193962E-03	8.465086E-02	9.451972E-05

Table 3a. Correlation Parameters. Four accelerometers at the middle plane.

.dat
 LO NASTRAN: 4 CONM2 (7 gr.) en el plano medio de la placa
 QUAD4 V67.5
 Lumped mass matrices
 : 4 acel.

 P A R A M E T R O S D E C O R R E L A C I O N
 P A R A
 5 MODOS EXPERIMENTALES Y
 6 MODOS ANALITICOS

TEST NO. 1, FRECUENCIA (HZ) = 2.969900E+02

ANAL. NO.	MAC	MAC GST	MAC GPS	NCO	SCO
1	9.950361E-01	4.600340E-03	3.362207E-03	2.439876E-04	6.635846E-06
2	1.306029E-03	5.073657E-01	9.108389E-01	2.239213E-01	1.633428E-02
3	2.465913E-04	1.180269E-01	1.380179E-05	7.561985E-06	4.859051E-03
4	1.304335E-03	1.715275E-01	6.895114E-02	2.828289E-05	3.231737E-02
5	2.668564E-05	1.320640E-02	1.135480E-03	5.845185E-04	2.357057E-02
6	8.165166E-06	4.844727E-02	4.815101E-02	3.229792E-03	9.972141E-01

TEST NO. 2, FRECUENCIA (HZ) = 3.493000E+02

ANAL. NO.	MAC	MAC GST	MAC GPS	NCO	SCO
1	1.037602E-02	7.541145E-08	3.285887E-03	2.379311E-04	2.470309E-05
2	9.681224E-01	4.612482E-01	9.113292E-01	2.234986E-01	1.503085E-02
3	1.164749E-04	2.267978E-01	8.531794E-06	5.645972E-06	5.756386E-03
4	9.681564E-01	7.668345E-02	6.854140E-02	2.417722E-05	3.048299E-02
5	4.796105E-05	4.981924E-03	1.089990E-03	5.632766E-04	2.179649E-02
6	5.105079E-05	1.665848E-02	4.800896E-02	3.220452E-03	9.964549E-01

Table 3b. Correlation Parameters. Four accelerometers at real location.

r.dat
 LO NASTRAN: 4 RBAR de 13 mm
 4 CONM2 (7 gr.) en el extremo de las RBAR
 QUAD4 V67.5
 Lumped mass matrices
 : 4 acel.

 P A R A M E T R O S D E C O R R E L A C I O N

P A R A
 5 MODOS EXPERIMENTALES Y
 6 MODOS ANALITICOS

TEST NO. 1, FRECUENCIA (HZ) = 2.969900E+02

ANAL. NO.	MAC	MAC GST	MAC GPS	NCO	SCO
1	9.845527E-01	5.518700E-03	4.675435E-03	3.563505E-04	9.939403E-01
2	1.354293E-03	4.287262E-01	8.854904E-01	2.633898E-01	3.976075E-06
3	2.387971E-04	1.302080E-01	2.026182E-03	2.393106E-04	2.351854E-04
4	1.390268E-03	1.929948E-01	8.594116E-02	6.551497E-04	1.749703E-03
5	5.548844E-05	1.262192E-02	3.359903E-04	6.278479E-04	1.281497E-04
6	3.073110E-05	5.376031E-02	6.143237E-02	5.332783E-03	3.942675E-03

TEST NO. 2, FRECUENCIA (HZ) = 3.493000E+02

ANAL. NO.	MAC	MAC GST	MAC GPS	NCO	SCO
1	1.013536E-02	1.357223E-06	4.643737E-03	3.655661E-04	8.204793E-03
2	9.281631E-01	4.034123E-01	8.849300E-01	2.637680E-01	1.107566E-03
3	1.412972E-04	2.417950E-01	1.249266E-03	1.317643E-04	1.518268E-04
4	9.547955E-01	8.554906E-02	8.720641E-02	6.905442E-04	9.832236E-01
5	3.123470E-05	5.086957E-03	3.851177E-04	6.425555E-04	1.301981E-06
6	2.004191E-04	1.597245E-02	6.234480E-02	5.416763E-03	7.310909E-03

Maximum of MAC and SCO are in bold letters. Result indicates that locate the accelerometers in the actual position is advantageous for the correlation. Also, SEREP expansion process seems to be the best expansion technique for this example.

Figure 2 compares the analytical mode versus the experimental expanded mode. Plot has been performed with XL v3B.

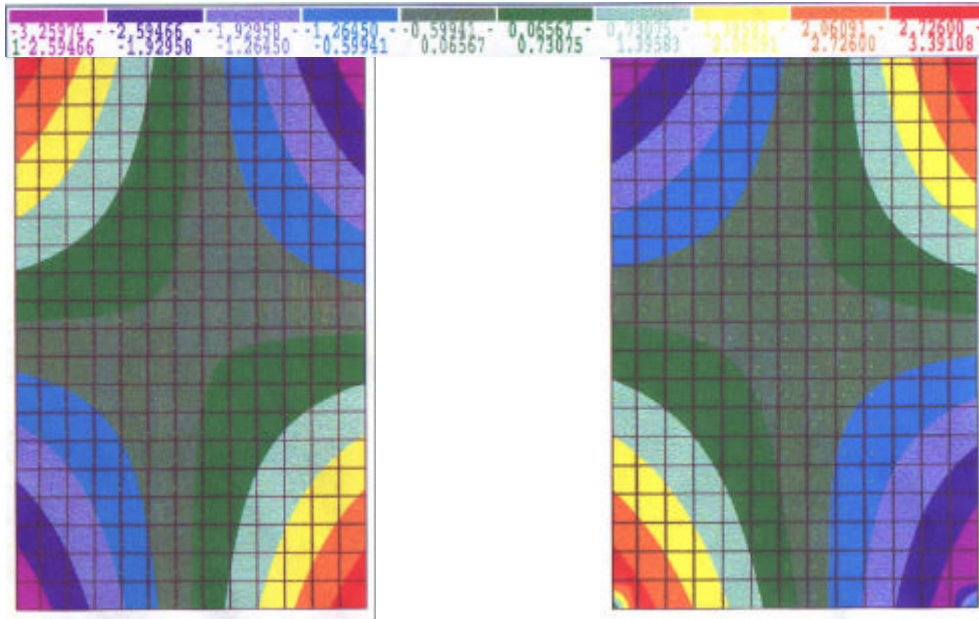


Figure 2 On the left, the first mode shape calculated by finite element model. On the right the experimental mode expanded by SEREP.

Figure 3 compares the mass error vector. Plots correspond to the error vector calculated based on three models: without including the accelerometers' mass; concentrated mass on the grids in the middle plane; concentrated mass on the tip of rigid bars to connect the actual accelerometer position to the nearest grid point. It shows the convenience of including the accelerometers and the benefit of modifying their location.

V. Polar Platform Panel

Finally, figure 4 shows the error mass and stiffness vectors plotted when the presented procedure was applied to the model of the Polar Platform Panels⁹. Mass error vector distribution shows that error is concentrated on the brackets joining the panel to the fixture. Including their influence matrix performed the structural model of these elements. This fact could explain that errors seem to be concentrated on these grids. Stiffness error matrix presents high values in the attachment of the fixture to the soil.

VI. Conclusions

A tool developed on MSC/NASTRAN v68.2 is presented. This tool helps to correlate tests and analysis. The main benefit is that expanded modes and error vectors are plotted on the structure, and, then, an user friendly decision tool can be used to modify the finite element model.

VI. Acknowledgement

Authors want to thank the collaboration of C.A.S.A. Space Division. Their engineers performed the test and the finite element model. Authors want to thank Dr. Kimon Alexiou for helpful discussions.

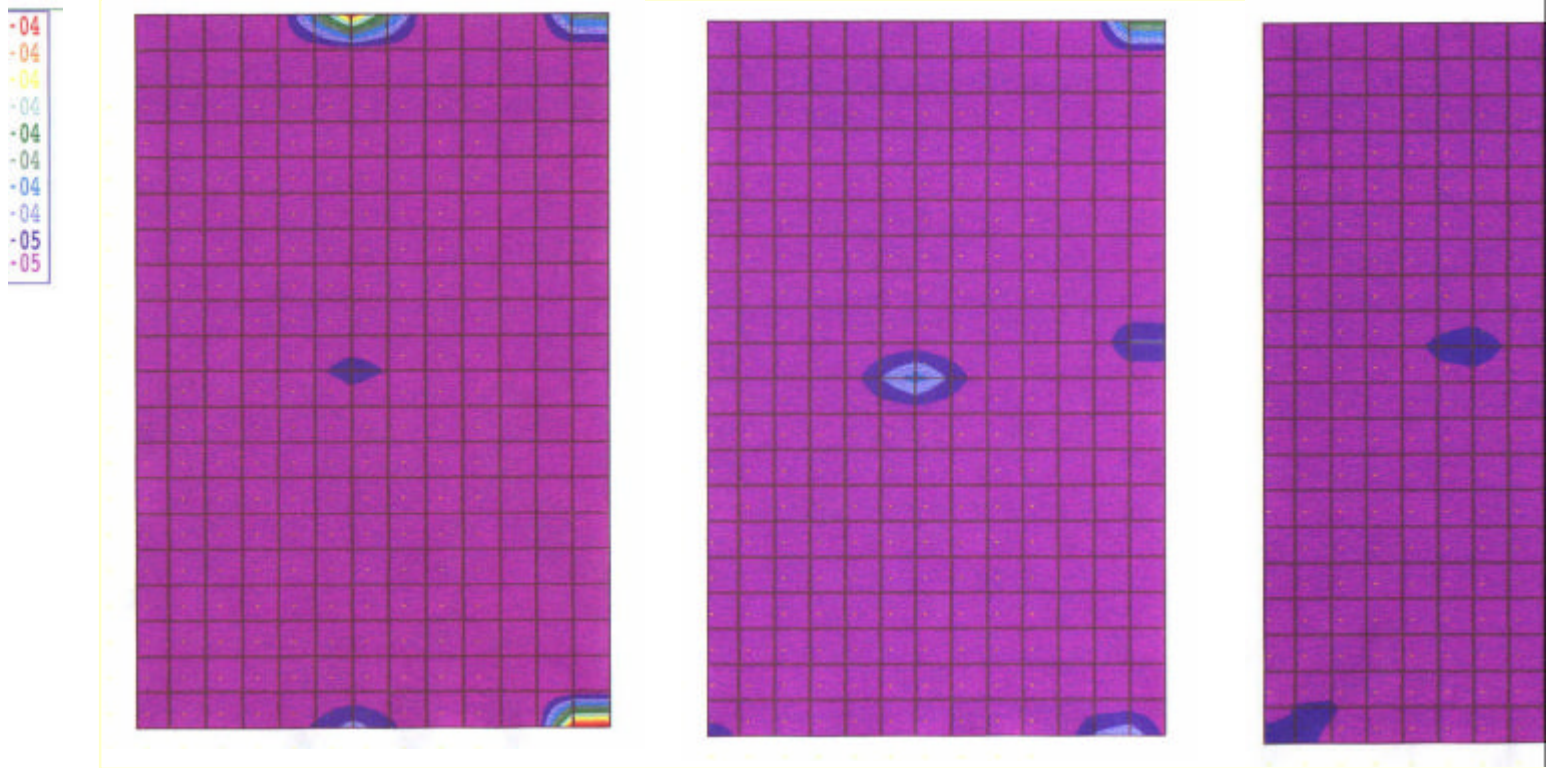


Figure 3 In the left, error \vec{v} calculated for the mass matrix when accelerometers mass is not taken into account. In the middle, accelerometer mass is assigned to nearest grid point. In the right, rigid bars are used to simulate the real I

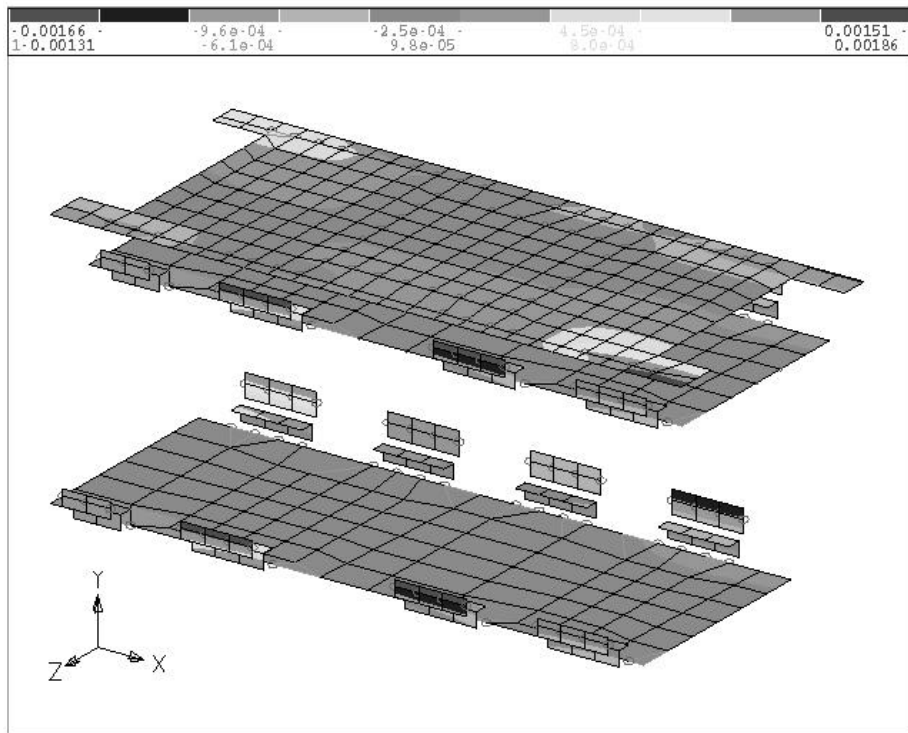


Fig. 4a Distribution of Mass Error Vector on the Polar Platform Panel

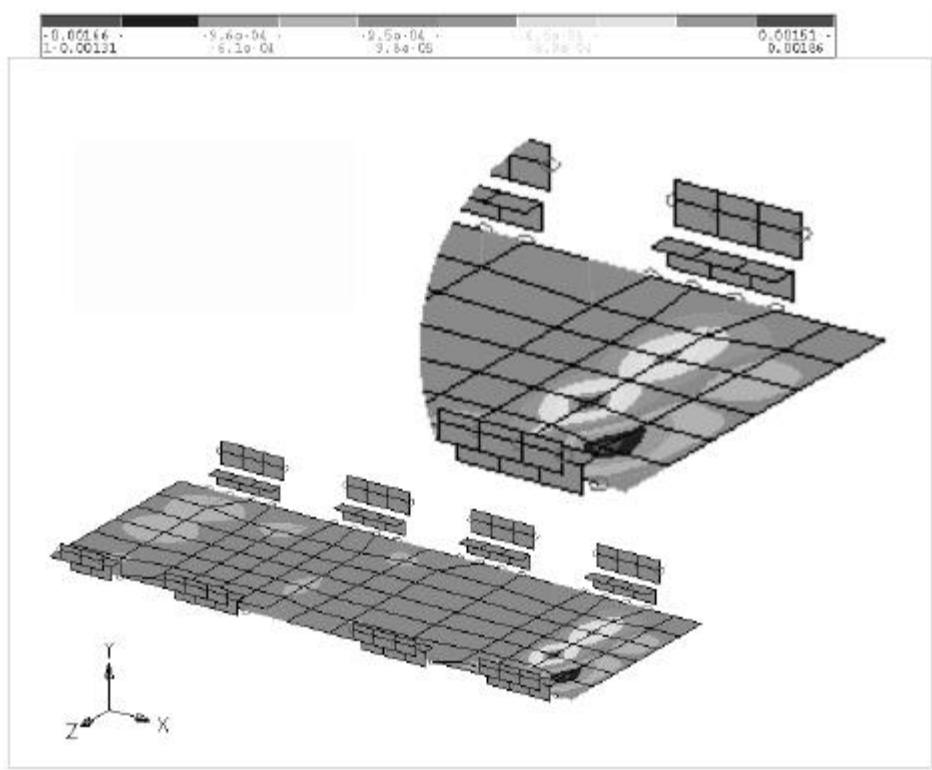


Fig. 4b Distribution of Stiffness Error Vector on the Polar Platform Panel

VII References

- ¹ Friswell, M.I. and Mottershead, J.E., *Finite Element Model Updating in Structural Dynamics*, Kluwer Academic Publishers, 1995.
- ² Imregun, M. And Visser, W.J., "A review of model updating techniques", *Shock and Vibration Digest*, Vol. 23, No. 1, 1991, pp. 9-20.
- ³ Ibrahim, S. R., "Correlation and updating methods: finite element dynamic model and vibration test data", *Proceedings of the DTA/NAFEMS International conference on structural dynamics modelling*, National Agency for Finite Elements Methods and Standards, Birmiehill East Killbride, Glasgow, Scotland, UK, 1993, pp. 323-347.
- ⁴ Denoyer, K. K. and Peterson L. D., "Model update using modal contribution to static flexibility error", *AIAA Journal*, Vol. 35, No. 11, 1997, pp. 1739-1744.
- ⁵ Denoyer, K. K. and Peterson L. D., "Comparing model update error residuals and effects on model predictive accuracy", *AIAA Journal*, Vol. 36, No. 10, 1998, pp. 1894-1900.
- ⁶ López-Díez, J. and Marco-Gómez, V., "Implementación de nuevas técnicas de localización y visualización de errores en modelos de elementos finitos de gran tamaño", *Actas de la 3ª Conferencia de Usuarios de MSC en España*, MacNeal Ibérica, S.L, 1997.
- ⁷ Möller, P. W. And Friberg, O., "Updating large finite element models in structural dynamics", *AIAA Journal*, Vol. 36, No. 10, 1998, pp. 1861-1868.
- ⁸ López-Díez, J., Marco-Gómez, V. and Luengo, P., "modal effective mass applied to error localization of finite element models", *Proceeding of the 20th Structural Dynamics and Materials Conference*, AIAA Paper No. 99-1310, St. Louis 1999.
- ⁹ Marco-Gómez, V., López-Díez, J. and Luengo, P., "Improvement of FE Analytical Models of Structures using Modal Testing Data", *Proceeding of the CEAS International Forum on Aeroelasticity and Structural Dynamics*, Vol. 3, 1997, pp. 307-314.
- ¹⁰ Ewins, D., *Modal Testing: Theory and Practice*, Research Studies Press, Letchworth, Herdfordshire, England, 1984.
- ¹¹ Sambasiva Rao, M., Nair, P. S. And Durvasula, S., "Equivalent Dynamic Models for a Spacecraft and its Subsystems", *ESA Journal*, Vol. 10, No. 1, 1986, pp. 93-111.
- ¹² Allemang, R. J. and Brown, D. L., "A correlation coefficient for modal vector analysis" *1st International Modal Analysis Conference*, pp. 110-116. 1982.
- ¹³ Ewins, D. J. and Sidhu, J., "Correlation of finite elements and modal test studies of practical structures" *2nd International Modal Analysis Conference*, 1984.
- ¹⁴ Imamovic, N. and Ewins, D.J., "An Automatic Correlation Procedure for Structural Dynamics", *CEAS International Forum on Aeroelasticity and Structural Dynamics*, pp. 56.1-56.12, 1995
- ¹⁵ Noor, A. K. "Recent advances and applications of reduction methods", *Appl. Mech. Rev. Vol 47, No 5*, pp. 127-146, 1994.
- ¹⁶ Guyan, R.J., "Reduction of stiffness and mass matrices", *AIAA Journal*, Vol. 3, No. 2, 1965, pp. 380.
- ¹⁷ Kidder, R.L., "Reduction of structural frequency equations", *AIAA Journal*, Vol. 11, No. 6, 1973, pp. 892.
- ¹⁸ Miller, C.A., "Dynamic reduction of structural models". *Journal of the Structural Division*, Vol. 106, No. ST10, 1980, pp. 2097-2108.
- ¹⁹ Paz, M., "Dynamic condensation", *AIAA Journal*, Vol 22, No. 5, 1984, pp. 724-727.
- ²⁰ Suarez, L. E. And Shing, M. P., "Dynamic condensation method for structural eigenvalue analysis", *AIAA Journal*, Vol. 30, No. 4, 1992, pp. 1046-1054.
- ²¹ O'Callahan, J., "A procedure for an Improved Reduced System (IRS) model", *7th International Modal Analysis Conference*, Las Vegas, Nevada, Feb. 1989, pp. 17-21.
- ²² Kodiyalam, S., Kao, P. and Wang, G., "Analysis and test correlation of spacecraft structures using dynamic parameter sensitivities", *AIAA Journal*, Vol. 32, No. 11, 1994, pp. 2286-2292.
- ²³ Kammer, D.C., "Test-analysis model development using an exact model reduction", *Int. J. of Analytical and Experimental Modal Analysis*, Vol. 2, No. 10, 1987, pp 174-179.
- ²⁴ O'Callahan, J., Aavailable, P. and Rimer, R., "System equivalent reduction expansion process", *Proceedings of the 7th International Modal Analysis Conference*, Las Vegas, 1989, pp 17-21.
- ²⁵ Kammer, D.C., "A hybrid approach to test-analysis-model development for large space structures", *Journal of Vibrations and Acoustics*, Vol. 113, 1991, pp 325-332.

-
- ²⁶ Kim, K. O., "Improved hybrid dynamic condensation for eigenproblems", AIAA Paper 96-1401, April 1996.
- ²⁷ Papadopoulos, M. and García, E, "Improvement in model reduction schemes using the system equivalent reduction expansion process", *AIAA Journal*, Vol. 34, No. 10, 1996, pp. 2217-2219.
- ²⁸ Qu, Z. and Fu, Z. "Comment on improvement in model reduction schemes using the system equivalent reduction expansion process", *AIAA Journal*, Vol. 36, No. 10, 1998, pp. 1941.
- ²⁹ Papadopoulos, M. and García, E, "Reply to Qu and Fu", *AIAA Journal*, Vol. 34, No. 10, 1996, pp. 1941-1942.
- ³⁰ Flanigan, C. C., "Implementation of the IRS dynamic reduction method in MSC/Nastran". *The MSC 1990 World users' conference proceedings*. Vol. I, Paper No. 13. 1990
- ³¹ Chung, Y. T., "Model reduction and model correlation using MSC/NASTRAN" *The MSC 1995 World users' conference proceedings*. Paper No. 8. 1995
- ³² Baruch, M., "Parametric methods of reference basis for the identification of linear dynamic structures", *35th Israel annual conference on aerospace science*, 1995.
- ³³ Blevins, R. D., *Formulas for natural frequency and mode shape*. Krieger Publishing Company, Malabar, Florida, 1993.